

Analytical Optimization of the Net Residual Dispersion in SPM-Limited Dispersion-Managed Systems

Xiaosheng Xiao, Shiming Gao, Yu Tian, and Changxi Yang

Abstract—Dispersion management is an effective technique to suppress the nonlinear impairment in fiber transmission systems, which includes tuning the amounts of precompensation, residual dispersion per span (RDPS), and net residual dispersion (NRD) of the systems. For self-phase modulation (SPM)-limited systems, optimizing the NRD is necessary because it can greatly improve the system performance. In this paper, an analytical method is presented to optimize NRD for SPM-limited dispersion-managed systems. The method is based on the correlation between the nonlinear impairment and the output pulse broadening of SPM-limited systems; therefore, dispersion-managed systems can be optimized through minimizing the output single-pulse broadening. A set of expressions is derived to calculate the output pulse broadening of the SPM-limited dispersion-managed system, from which the analytical result of optimal NRD is obtained. Furthermore, with the expressions of pulse broadening, how the nonlinear impairment depends on the amounts of precompensation and RDPS can be revealed conveniently.

Index Terms—Dispersion management, net residual dispersion (NRD), optical fiber communication, self-phase modulation (SPM).

I. INTRODUCTION

IN LONG-HAUL transmission systems, amplified spontaneous emission (ASE) noise cumulates along the transmission link and degrades the system performance. In order to ensure a sufficient optical signal-to-noise ratio at the receiver (Rx), the launch power has to be increased. With a high signal power, the nonlinear fiber effects severely degrade the system performance. One of the effective techniques to reduce nonlinear impairment is through the use of the dispersion management technique [1]–[3], which includes careful tuning of the amount of group velocity dispersion (GVD) 1) directly after the transmitter (Tx) (precompensation), 2) within the repeaters (in-line compensation), and 3) directly before the Rx (postcompensation), as illustrated in Fig. 1. The corresponding three quantities, i.e., the amounts of precompensation, residual

dispersion per span (RDPS), and net residual dispersion (NRD), are key parameters for designing a transmission system with high performance. The NRD is defined as the cumulated GVD at the end of the link. In a “pseudolinear” system [4], [5], the optimal NRD is around zero. For this kind of system, in which the bit rate is very high and the signal is usually modulated as return-to-zero pulse with small duty cycle, the dominant nonlinearities are intrachannel nonlinear effects. However, in self-phase modulation (SPM)-limited systems, it was found that a positive NRD can greatly improve the system performance [3], [6] and that the amount of optimal NRD increases with the input signal power and the number of repeat fiber spans.

In order to suppress the nonlinearities mostly by dispersion management, the amounts of GVD compensations of the system should be optimized. Numerical simulation is an accurate method to optimize the system; however, its intrinsic shortcoming is time consuming, especially for a new system design with multiparameters. Therefore, simple and fast methods for first-order system design are necessary. Some simple design rules have been proposed to optimize the dispersion map for various systems [3], [4], [7]–[9]. Through numerical simulations, Frignaca and Bigo found that the optimal NRD is proportional to the nonlinear phase [3]. Some groups proposed simple rules to optimize the precompensation or in-line compensation [4], [7]–[9]. Unfortunately, analytical models for optimizing the amounts of NRD have not been reported yet. In this paper, we present an analytical method to optimize the NRD for SPM-limited dispersion-managed systems. By use of this method, the dependence of the nonlinear impairment on the amounts of precompensation and RDPS can also be easily found.

The principle of this method is based on the correlation between the nonlinear impairment and the output pulse broadening in SPM-limited systems. The performance of dispersion-managed systems can be optimized through minimizing the output single-pulse broadening. Yu and Fan have derived approximate analytical formulas to calculate the pulse width evolution in chained optical amplifier systems [10]. Based on the analytical method developed by Yu and Fan [10], we found that the relation between the square of the output pulse width and the NRD is parabolic for an SPM-limited system. Afterward, a set of relative simple expressions for output pulse width is derived. With these expressions, the dependence of the output pulse width, thus the nonlinear penalty, of the SPM-limited dispersion-managed system on precompensation, RDPS, and NRD can be evaluated.

Manuscript received August 4, 2005; revised January 5, 2006. This work was supported in part by the National Natural Science Foundation of China under Grant 60478003 and the Specialized Research Fund for the Doctoral Program of Higher Education (SRFDP) under Grant 20040003064.

The authors are with the State Key Laboratory of Precision Measurement Technology and Instruments, Department of Precision Instruments, Tsinghua University, Beijing 100084, China (e-mail: xiaoxsh98@mails.tsinghua.edu.cn; gaosm@mail.tsinghua.edu.cn; tianyu03@mails.tsinghua.edu.cn; cxyang@tsinghua.edu.cn).

Digital Object Identifier 10.1109/JLT.2006.872278

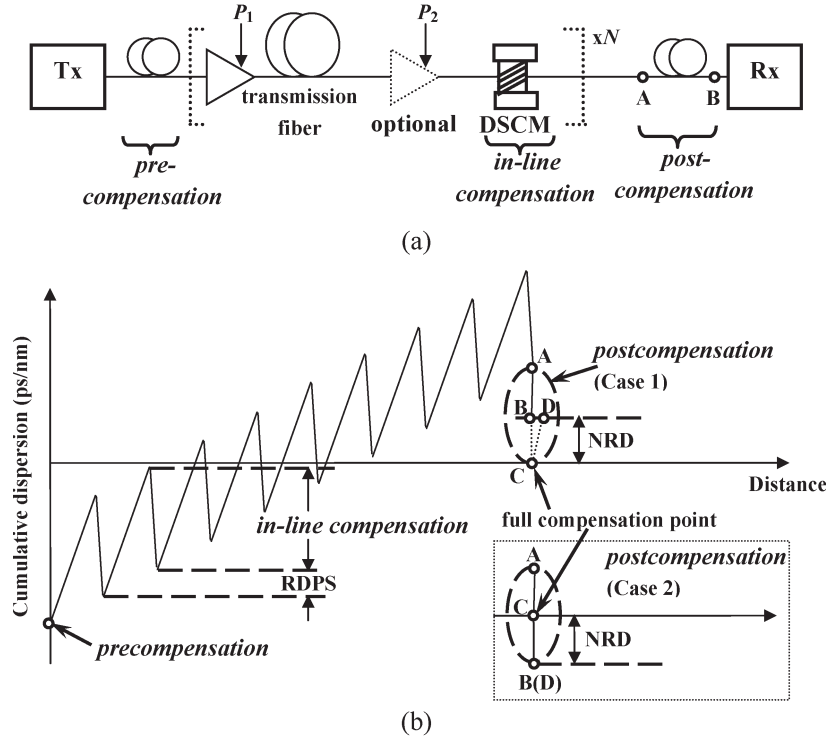


Fig. 1. (a) System set-up and (b) the corresponding dispersion map. The inset in (b) indicates another case of postcompensation. P_1 : output power of the first EDFA; P_2 : output power of the second EDFA (optional).

The remainder of this paper is organized as follows. The principle of the optimization method is presented in Section II. In Section III, a set of analytical results of pulse broadening is derived to optimize the NRD, and our analytical results are compared with numerical simulations. Section IV presents the discussion and conclusion.

II. PRINCIPLE OF THE OPTIMIZATION METHOD

In this section, we will discuss the principle of the optimization method, i.e., the correlation between the nonlinear impairment and the output pulse broadening of SPM-limited systems. For systems dominated by the SPM effect, the combined effect of SPM and dispersion results in pulse amplitude fluctuations, which distort the output pulse and degrade the system performance. On the other hand, the main effect of SPM can also be regarded as to induce an effective frequency chirp to the input pulse, which alters the broadening rate imposed on the pulse by the GVD alone [11], [12]. Therefore, one can use the output single-pulse broadening to evaluate the nonlinear impairment of SPM-limited systems. In [12], the authors have shown that the output single-pulse broadening gives a good evaluation of the eye-opening penalty (EOP) of an SPM-limited system when waveform distortion is small. Here, we further show that in an SPM-limited system, the dispersion map optimizing the system performance matches that minimizing the output pulse broadening, even taking account of the ASE noise.

The system setup is illustrated in Fig. 1(a), which consists of an ideal electrical Tx, precompensation, N transmission spans periodically amplified by in-line optical amplifiers, post-compensation, and an Rx. The Tx includes a power booster

and the Rx includes a preamplifier, optical filter, square law detector, and electrical filter. The in-line amplification schemes could be single-stage erbium-doped fiber amplifier (EDFA), double-stage EDFA, or hybrid EDFA–Raman amplification. Each transmission span is made of a transmission fiber followed by dispersion and full dispersion slope compensation module (DSCM). The DSCM could be a dispersion-compensating fiber (DCF) or a fiber grating. The corresponding dispersion map is shown in Fig. 1(b). It should be noted that the signs of the pre-compensation, RDPS, and NRD could be positive or negative. In the following simulations, a 10-Gb/s single-channel system shown in Fig. 1 is considered, in which the input signal is the unchirped nonreturn-to-zero (NRZ) pulse, the amplification scheme is chosen as a double-stage EDFA, and the DSCM is DCF. However, the results are valid to all possible SPM-limited systems.

Fig. 2 shows the system impairments with different amplifier noise figures (NFs) and the output single-pulse broadening factor versus the NRD of the system. The nonlinear impairment is represented by EOP, which is calculated by $EOP = 10 \log_{10}(EO_{b2b}/EO_{tr})$, where EO_{b2b} and EO_{tr} are the back-to-back eye opening and the eye opening after transmitting the whole link, respectively. The eye opening is defined as the height of the highest rectangular mask with a 20% bit width that can be inserted inside the eye diagram. The EOP is obtained by solving the nonlinear Schrödinger equation with split-step Fourier method [11], and a pseudorandom binary sequence of $2^7 - 1$ bits is used. ASE noise is modeled as a complex zero-mean additive white Gaussian noise (AWGN) in the numerical simulations. The NRZ signal is represented by an m th-order super-Gaussian shape pulse with

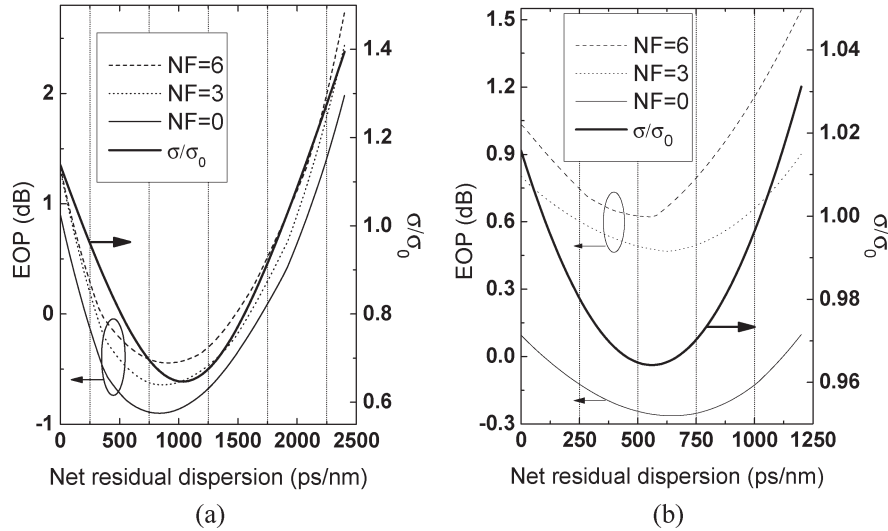


Fig. 2. EOP (with different amplifier NFs) and single-pulse broadening factor σ/σ_0 versus the NRD corresponding to a system with (a) $P_1 = 3$ dBm, $P_2 = 0$ dBm, and (b) $P_1 = -3$ dBm, $P_2 = -6$ dBm. The precompensation and RDPS of the transmission link are -700 and 50 ps/nm, respectively. All the data are obtained from numerical simulations.

$m = 1.436$. In the Rx, the optical filter is simulated by a second super-Gaussian filter with a bandwidth of two times the data rate, and the electrical filter is represented by a Bessel filter with a bandwidth of 70% of the data rate. The single-pulse broadening factor is described by σ/σ_0 , where σ and σ_0 are the root mean square (rms) width of the output and input pulse, respectively. When calculating the output pulse width σ , the effects of ASE noise and filters on the pulse width are all neglected. The broadening factor σ/σ_0 in Fig. 2 is obtained by numerical simulations. The simulation parameters of the transmission fiber are span number $N = 10$, length $L_1 = 80$ km, attenuation $\alpha_1 = 0.2$ dB/km, nonlinear coefficient $\gamma_1 = 1.317$ W⁻¹km⁻¹, dispersion $D_{21} = 17$ ps/km/nm, and dispersion slope $D_{31} = 0.056$ ps/km/nm², and for DSCM (here it is DCF) are $\alpha_2 = 0.5$ dB/km, $\gamma_2 = 5.27$ W⁻¹km⁻¹, and $D_{22} = -100$ ps/km/nm. The dispersion slope of the DCF is adaptive to fully compensate for that of the transmission fiber. The length of DCF is determined by the amount of RDPS. The amounts of precompensation and RDPS of the transmission link considered in Fig. 2 are -700 and 50 ps/nm, respectively. The nonlinearities of the precompensation and postcompensation segments are neglected. In Fig. 2(a), the average input powers of the first and second EDFAs are $P_1 = 3$ dBm (launch power of transmission fiber) and $P_2 = 0$ dBm (launch power of DSCM), respectively. In order to emphasize the impact of ASE on system performance, systems with much weaker signal powers, i.e., $P_1 = -3$ dBm and $P_2 = -6$ dBm, are considered in Fig. 2(b). Other parameters in Fig. 2(b) are the same as Fig. 2(a). From Fig. 2, it can be seen that with the increase of NRD from 0 to 2400 ps/nm [Fig. 2(a)] or from 0 to 1200 ps/nm [Fig. 2(b)], the EOP decreases at first, then reaches its minimum, and finally increases monotonously. We note that the location of the EOP minimization is almost the same as that of the minimization of the output pulse broadening factor, which is independent of the NF level of the amplifier. Hence, the ASE noise is neglected in following simulations.

III. THEORETICAL DERIVATION AND THE OPTIMIZATION OF DISPERSION

Now we derive the analytical expression of the pulse broadening factor. Focusing on the impact of NRD on the pulse broadening, the dispersion map can be divided into two parts. One is the full compensation part and the other is the NRD part, as shown in Fig. 1(b). For the full compensation part, the dispersion is fully compensated, which is indicated by the part from the starting point of the link to the full compensation point C in Fig. 1(b). The NRD part is shown as the CD segment. If the cumulative dispersions along the postcompensation (AB) segment are always positive or negative, there is no intersection between AB and the horizontal axis, such as the case 1 shown in Fig. 1(b). In this case, the postcompensation segment can be replaced by the ABCD segment. The ABCD segment consists of the postcompensation (AB) and two additional dispersion compensators (BC and CD), where the two additional compensators are linear and the sum of the cumulative dispersion is exactly equal to zero. Therefore, in this case, the output pulse at the B point is exactly the same as that of the D point. For another case shown in the inset of Fig. 1(b) (case 2), the postcompensation is divided into two segments, AC and CB(D), where AC belongs to the full compensation part and CB(D) acts as the NRD part. In both cases, the signal power at the NRD part (i.e., CD segment) is generally very weak, thus the nonlinear effect of that part can be neglected.

Neglecting the effect of dispersion slope and ASE noise, using the method developed in [10], the squared rms width of the output pulse is described as

$$\langle \tau^2 \rangle = \langle \tau^2 \rangle^L + \langle \tau^2 \rangle_2^{NL} + \langle \tau^2 \rangle_3^{NL} + \langle \tau^2 \rangle_{41}^{NL} + \langle \tau^2 \rangle_{42}^{NL} \quad (1)$$

where $\langle \tau^2 \rangle = \sigma^2$, $\langle \tau^2 \rangle^L$ is the linear term caused only by the chromatic dispersion of the fiber. In order to obtain accurate results, the nonlinear parts resulting from the SPM effect are expanded to the fourth order, where $\langle \tau^2 \rangle_2^{NL}$, $\langle \tau^2 \rangle_3^{NL}$, and

$\langle \tau^2 \rangle_{41}^{NL} + \langle \tau^2 \rangle_{42}^{NL}$ are the second-, third-, and fourth-order nonlinear terms, respectively. The first-order nonlinear term is zero, and for an initially unchirped pulse input, $\langle \tau^2 \rangle_3^{NL} \equiv 0$. The second part of the fourth-order nonlinear term $\langle \tau^2 \rangle_{42}^{NL}$ is not considered in the simulations of Yu and Fan [10]. It is necessary to take this term into account here because it is important for cases with large precompensation or RDPS. The squared rms width after transmitting through the full compensation part (i.e., at point C) is described as

$$\langle \tau^2 \rangle|_{z=C} = \langle \tau^2 \rangle^L|_{z=C} + \langle \tau^2 \rangle_2^{NL}|_{z=C} + \langle \tau^2 \rangle_{41}^{NL}|_{z=C} + \langle \tau^2 \rangle_{42}^{NL}|_{z=C} \quad (2)$$

where the first three terms on the right-hand side (RHS) could be simplified to those shown in [10, eqs. (A.7), (A.31), and (A.33)]. The fourth term on the RHS is described as fourfold integrals in [10, eq. (A.22)], which is too complex to having an analytical result. For the system with zero overall dispersion, we simplify it to

$$\langle \tau^2 \rangle_{42}^{NL}|_{z=C} = 3a_{42}|Nggg\rangle$$

where $|Nggg\rangle = \int_0^{L_0} N(z) [\int_0^z G(x) dx]^3 dz$ is a twofold integral and its analytical expression can be much simpler for a uniform dispersion-managed system in which the N cascaded spans of transmission link are all the same. Then (2) is given by

$$\langle \tau^2 \rangle|_{z=C} = b_0 - a_2|Ng\rangle + a_{41} \left(2|Nngg\rangle - \frac{1}{2}|Ng\rangle^2 \right) + 3a_{42}|Nggg\rangle \quad (3)$$

where $|Ng\rangle = \int_0^{L_0} N(z) [\int_0^z G(x) dx] dz$ and $|Nngg\rangle = \int_0^{L_0} N(z) [\int_0^z N(x) dx] [\int_0^z G(x) dx]^2 dz$ are both twofold integrals, and the coefficients b_0 , a_2 , a_{41} , and a_{42} are shown in [10] for an arbitrary input pulse (note that in the expressions of these coefficients in [10], “ E_0 ” in the denominator out of the integral should be 1). It should be noted that $\langle \tau^2 \rangle|_{z=C}$ does not depend on the NRD.

The increments of all the terms on the RHS of (1) resulting from the additional NRD part [CD segment of Fig. 1(b)] are simplified to

$$\langle \tau^2 \rangle^L|_{z=C \rightarrow D} = b_2 R^2 \quad (4)$$

$$\langle \tau^2 \rangle_2^{NL}|_{z=C \rightarrow D} = a_2 |N\rangle R \quad (5)$$

$$\langle \tau^2 \rangle_{41}^{NL}|_{z=C \rightarrow D} = a_{41} \left(|N\rangle |Ng\rangle R - 4|Nng\rangle R + \frac{1}{2}|N\rangle^2 R^2 \right) \quad (6)$$

$$\langle \tau^2 \rangle_{42}^{NL}|_{z=C \rightarrow D} = a_{42} (-5|Ngg\rangle R + 2|Ng\rangle R^2) \quad (7)$$

where $|N\rangle = \int_0^{L_0} N(z) dz$, $|Nng\rangle = \int_0^{L_0} N(z) [\int_0^z N(x) dx] [\int_0^z G(x) dx] dz$, $|Ngg\rangle = \int_0^{L_0} N(z) [\int_0^z G(x) dx]^2 dz$, $R = \int_C^D \beta_2(z)/T_0^2 dz$ represents the cumulative dispersion of the

NRD part, and T_0 is the half width at $1/e$ intensity point. The terms including R in (4)–(7) show the impact of NRD on the pulse broadening. Substituting (3)–(7) into (1), the pulse width after transmitting through the whole link (at point D), including the full compensation part and the NRD part, is obtained as

$$\langle \tau^2 \rangle = \langle \tau^2 \rangle|_{z=C} + bR + aR^2 \quad (8)$$

where $b = a_2|N\rangle + a_{41}|N\rangle|Ng\rangle - 4a_{41}|Nng\rangle - 5a_{42}|Ngg\rangle$ and $a = b_2 + (1/2)a_{41}|N\rangle^2 + 2a_{42}|Ng\rangle$. From (8), it can be seen that the relation between $\langle \tau^2 \rangle$ and R is a parabolic shape; thus, with tuning of the amounts of NRD, there only one extremum exists.

For an unchirped m th-order super-Gaussian shape pulse, the coefficients mentioned above are $b_0 = (1/m)\Gamma(3/2m)$, $b_2 = m\Gamma(2 - (1/2m))$, $a_2 = (1/m)2^{(-1/2m)}\Gamma(1/2m)$, $a_{41} = (8m/9)3^{(1/2m)}\Gamma(2 - (1/2m))$, and $a_{42} = -2^{-2+(3/2m)}(-1 + 2m)[(-2 + 2m)\Gamma(2 - (3/2m)) - m\Gamma(3 - (3/2m))]$, where Γ is Gamma function. Since, in general, the parameter a in (8) satisfies $a > 0$, then the optimal NRD can be obtained from (8) as

$$R_{\text{opt}} = -\frac{b}{2a} = -\frac{a_2|N\rangle + a_{41}|N\rangle|Ng\rangle - 4a_{41}|Nng\rangle - 5a_{42}|Ngg\rangle}{2b_2 + a_{41}|N\rangle^2 + 4a_{42}|Ng\rangle} \quad (9)$$

From (8), the pulse broadening factor σ/σ_0 is

$$\frac{\sigma}{\sigma_0} = \sqrt{\frac{\langle \tau^2 \rangle|_{z=C} + bR + aR^2}{b_0}} \quad (10)$$

from which the dependences of pulse broadening on precompensation, RDPS, and NRD are obtained. In order to check the accuracy of (10) and the contribution to σ/σ_0 of each term on the RHS of (1), the simulation and analytical results of σ/σ_0 for systems with different precompensation and RDPS are shown in Fig. 3. The legends in Fig. 3 represent the terms that are considered in the analytical calculation of σ . For example, $\langle \tau^2 \rangle^L + \langle \tau^2 \rangle_{2+41}^{NL}$ represents that only the term $\langle \tau^2 \rangle^L + \langle \tau^2 \rangle_2^{NL} + \langle \tau^2 \rangle_{41}^{NL}$ on the RHS of (1) is considered (note that the first- and third-order nonlinear terms are all equal to zero). For a system with precompensation of -700 ps/nm and RDPS of 50 ps/nm, as seen in Fig. 3(a), it shows that considering $\langle \tau^2 \rangle^L + \langle \tau^2 \rangle_{2+41}^{NL}$ is enough to represent the pulse width in this case. However, for large precompensation and RDPS, as shown in Fig. 3(b), the contribution of $\langle \tau^2 \rangle_{42}^{NL}$ on the pulse width should be taken into account.

Using (9), a simple analytical expression of the optimal NRD R_{opt} for an SPM-limited system can be easily obtained by integrating the twofold integrations, provided that the dispersion-managed system is uniform and all the other parameters are given. Fig. 4 compares R_{opt} obtained from the numerical simulations of minimizing EOP and from the simplified expression of (9). The curves in Fig. 4 correspond to transmission links with different RDPSs. It can be seen that, for general cases, the

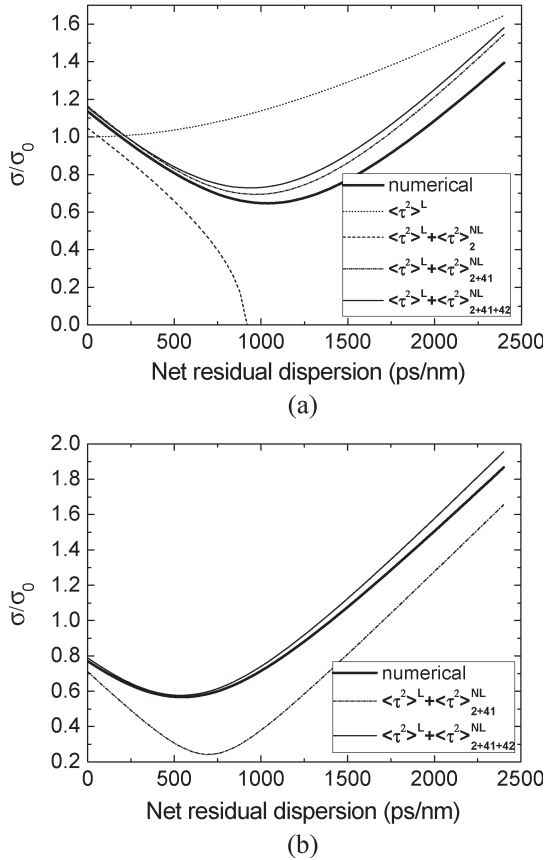


Fig. 3. Comparison of the numerical simulations and the analytical results of pulse broadening factor σ/σ_0 versus NRD. (a) System parameters are the same as Fig. 2(a). (b) Precompensation and RDPS of the link are -1500 and 100 ps/nm, respectively, and the other parameters are the same as Fig. 2(a). The legends with symbols represent the terms considered in the analytical calculation.

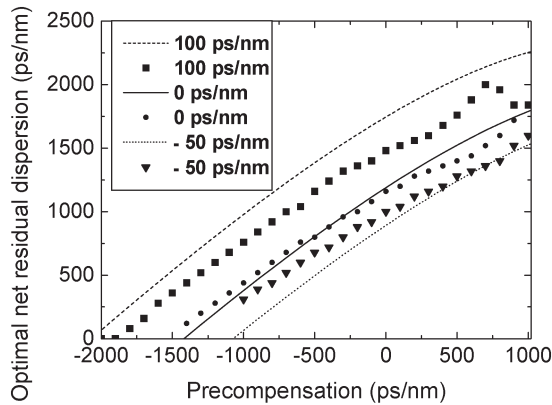


Fig. 4. Optimal NRD obtained from the numerical minimization of EOP (discrete dots) and from (9) (continuous curves) at different precompensations and RDPSs. The legends show the amounts of RDPSs. Other parameters of the systems are the same as Fig. 2(a).

optimal NRD obtained from (9) agrees well with that from the numerical simulation. When the magnitude of precompensation or RDPS is large, the accuracy of (9) deteriorates. However, the configurations with too large precompensation or RDPS exhibit high nonlinear penalties, which is not practical.

When designing a system that keeps the cumulative nonlinear phase shift [3], [13] approximately constant, one can

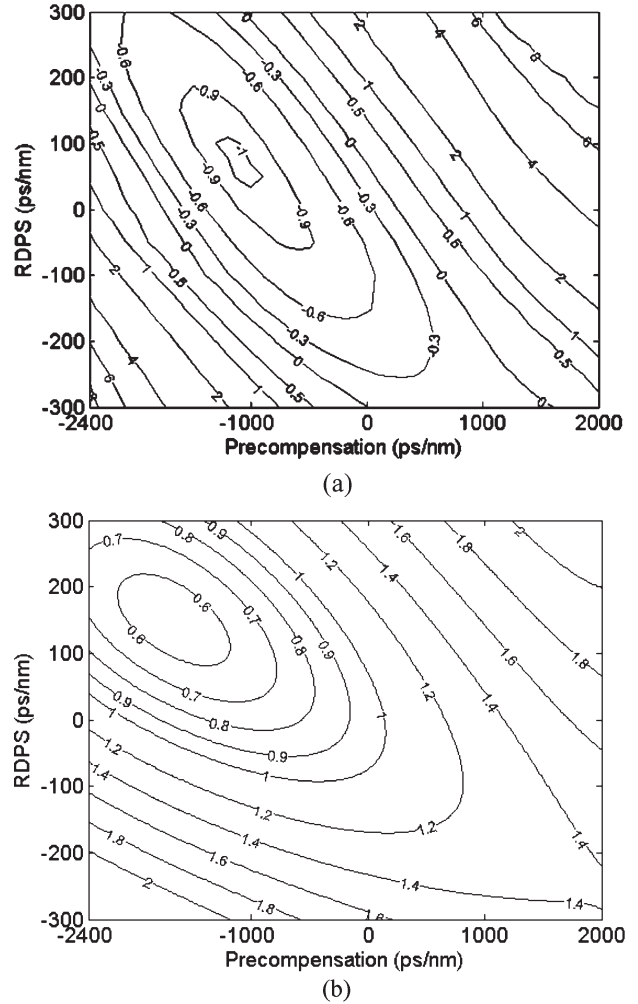


Fig. 5. Contour plots of (a) EOP and (b) pulse broadening factor σ/σ_0 versus precompensation and RDPS. Each point in the contours corresponds to the case when NRD is optimized. Other parameters of the systems are the same as Fig. 2(a).

obtain the approximate optimal values of precompensation, RDPS, and NRD by minimizing the pulse broadening factor σ/σ_0 . Substituting (9) into (10), the analytical expression of σ/σ_0 is obtained, which depends only on the precompensation and RDPS. Mathematically, the optimal precompensation and RDPS can be found first by minimizing σ/σ_0 with (10). Then, with the obtained precompensation and RDPS, the optimal NRD can be determined from (9). Fig. 5(a) and (b) shows the contour plots of the EOP and pulse broadening factor σ/σ_0 , respectively, versus precompensation and RDPS. Each point in the contours corresponds to the case that NRD is optimized. EOP is calculated by numerical simulation and σ/σ_0 is obtained by (9) and (10). As shown in Fig. 5, the trend of the nonlinear impairment with precompensation and RDPS obtained from analytical calculations approximately matches that from numerical simulations. The optimal values of precompensation, RDPS, and NRD from numerical simulations (analytical calculations) are -1080 (-1676), 60 (151), and 560 (672) ps/nm, respectively. The error of analytical results mainly comes from intrachannel four-wave mixing/cross-phase modulation. When the precompensation is very large, the distortion of a single

pulse is caused not only by a single-pulse SPM but also by other intrachannel nonlinear effects.

IV. DISCUSSION AND CONCLUSION

Compared to analytical models, numerical simulations are straightforward and precise for system design. For example, Xie recently used the numerical approach to optimize precompensation and NRD [14]. However, we think that the analytical models are meaningful. Equation (8) clearly shows that the relation between the SPM effect on signal pulse (represented by $\langle \tau^2 \rangle$) and the NRD (represented by R) is parabolic. For the NRZ format signal, the parameter a in (8) is $a = 1.3 + 0.84|N|^2 + 0.99|Ng|$, which was found to be positive in the general case. Thus, there exists one and only one local minimum EOP when tuning the NRD. Moreover, since $a > 0$, (9) indicates that the sign of the optimal NRD depends on b , and $R_{\text{opt}} > 0$ when $b < 0$. Since the sign of R_{opt} is the same as β_2 , the sign of the cumulative GVD (in picosecond per nanometer) is opposite the R_{opt} . Thus, the optimal NRD (in picosecond per nanometer) is negative in the case of $b < 0$. However, by using numerical simulations, [3] and [6] only show that the positive NRD can improve the system performance.

As an example, we consider the system in Fig. 4 with a fixing RDPS of 0 ps/nm to analyze the dependence of optimal NRD on precompensation. In this case, (9) is rewritten as

$$R_{\text{opt}} = -\frac{b}{2a} = -\frac{3.5 + 1.5 \times 10^{-3} \text{CD}_p - 0.70 \times 10^{-6} \text{CD}_p^2}{2(3.7 - 0.71 \times 10^{-3} \text{CD}_p)} \quad (11)$$

where CD_p is the cumulative dispersion of precompensation (in picosecond per nanometer). From the denominator of (11), it can be seen that $a < 0$ only when the precompensation is larger than 5200 ps/nm, which is too large to suppress the nonlinear effect. Meanwhile, the numerator shows that, when $\text{CD}_p < -1400$ ps/nm, b is less than zero; thus, the optimal NRD (in picosecond per nanometer) is negative in this case.

Equation (11) implicitly shows the influence of precompensation on the NRD. At the same time, the effect of precompensation on the nonlinear penalty can also be given by (8) or (10). For example, consider the system in Fig. 4 with both RDPS and NRD having a value of 0 ps/nm, the dependence of nonlinear pulse broadening on precompensation can be obtained as

$$\left(\frac{\sigma}{\sigma_0}\right)^2 = 2.1 + 1.9 \times 10^{-3} \text{CD}_p + 0.25 \times 10^{-6} \text{CD}_p^2 - 0.25 \times 10^{-9} \text{CD}_p^3.$$

In conclusion, the analytical expression of the optimal NRD for SPM-limited dispersion-managed systems has been obtained. The correlation between the SPM-limited system degradation (EOP) and the single-pulse broadening factor has been presented first, and then we obtained the expression of the optimal NRD through minimizing the pulse broadening. The analytical results have been verified by the numerical simulations through minimizing the EOP for dispersion-managed systems.

REFERENCES

- [1] A. Färbert, C. Scheerer, J.-P. Elbers, C. Glingener, and G. Fischer, "Optimized dispersion management scheme for long-haul optical communication systems," *Electron. Lett.*, vol. 35, no. 21, pp. 1865–1866, Oct. 1999.
- [2] A. Bertaina, S. Bigo, C. Francia, S. Gauchard, J.-P. Hamaide, and M. W. Chbat, "Experimental investigation of dispersion management for an 8×10 -Gb/s WDM transmission system over nonzero dispersion-shifted fiber," *IEEE Photon. Technol. Lett.*, vol. 11, no. 8, pp. 1045–1047, Aug. 1999.
- [3] Y. Frignaca and S. Bigo, "Numerical optimization of residual dispersion in dispersion-managed systems at 40 Gb/s," in *Proc. OFC*, Baltimore, MD, 2000, pp. 48–50.
- [4] R. I. Killey, H. J. Thiele, V. Mikhailov, and P. Bayvel, "Reduction of intrachannel nonlinear distortion in 40-Gb/s-based WDM transmission over standard fiber," *IEEE Photon. Technol. Lett.*, vol. 12, no. 12, pp. 1624–1626, Dec. 2000.
- [5] R.-J. Essiambre, G. Raybon, and B. Mikkelsen, "Pseudo-linear transmission of high-speed TDM signals: 40 and 160 Gb/s," in *Optical Fiber Telecommunications IV B*, I. Kaminow and T. Li, Eds. San Diego, CA: Academic, 2002.
- [6] C. Caspar, H.-M. Foisel, A. Gladisch, N. Hanik, F. Küppers, R. Ludwig, A. Mattheus, W. Pieper, B. Strebel, and H. G. Weber, "RZ versus NRZ modulation format for dispersion compensated SMF-based 10-Gb/s transmission with more than 100-km amplifier spacing," *IEEE Photon. Technol. Lett.*, vol. 11, no. 11, pp. 481–483, Apr. 1999.
- [7] J.-P. Elbers, A. Färbert, C. Scheerer, C. Glingener, and G. Fischer, "Reduced model to describe SPM-limited fiber transmission in dispersion-managed lightwave systems," *IEEE J. Sel. Topics Quantum Electron.*, vol. 6, no. 2, pp. 276–281, Oct. 2000.
- [8] Y. Frignac, J.-C. Antona, S. Bigo, and J.-P. Hamaide, "Numerical optimization of pre- and in-line dispersion compensation in dispersion-managed systems at 40 Gb/s," in *Proc. OFC*, Anaheim, CA, 2002, pp. 612–613.
- [9] Y. Frignac, J.-C. Antona, and S. Bigo, "Enhanced analytical engineering rule for fast optimization of dispersion maps in 40 Gb/s-based transmission systems," presented at the Optical Fiber Communication (OFC), Los Angeles, CA, 2004, Paper TuN3.
- [10] Q. Yu and C. Fan, "Analytical study on pulse broadening in chained optical amplifier systems," *J. Lightw. Technol.*, vol. 15, no. 3, pp. 444–451, Mar. 1997.
- [11] G. P. Agrawal, *Nonlinear Fiber Optics*, 3rd ed. San Diego, CA: Academic, 2001, ch. 4.
- [12] N. Kikuchi and S. Sasaki, "Analytical evaluation technique of self-phase-modulation effect on the performance of cascaded optical amplifier systems," *J. Lightw. Technol.*, vol. 13, no. 5, pp. 868–878, May 1995.
- [13] S. Vorbeck and M. Schneiders, "Cumulative nonlinear phase shift as engineering rule for performance estimation in 160-Gb/s transmission systems," *IEEE Photon. Technol. Lett.*, vol. 16, no. 11, pp. 2571–2573, Nov. 2004.
- [14] C. Xie, "A doubly periodic dispersion map for ultralong-haul 10- and 40-Gb/s hybrid DWDM optical mesh networks," *IEEE Photon. Technol. Lett.*, vol. 17, no. 5, pp. 1091–1093, May 2005.



Xiaosheng Xiao was born in Jishui, Jiangxi, China, in 1982. He received the B.E. degree from Tsinghua University, Beijing, China, in 2002 and is currently working toward the Ph.D. degree at the same university.

His research interests include nonlinear fiber optics and optical phase conjugation in optical fiber communications.



Shiming Gao was born in Heilongjiang, China, in 1977. He received the B.E. degree in machine design, manufacturing, and automation and the Ph.D. degree in optical engineering from Tsinghua University, Beijing, China, in 2000 and 2005, respectively. He is currently engaged in postdoctoral work at Tsinghua University.

His research interests include nonlinear optics, optical wavelength conversion, and nonlinearities in optical communication systems.



Yu Tian was born in Xi'an, China, in 1981. He received the B.E. degree from Tsinghua University, Beijing, China, in 2003 and is currently working toward the Ph.D. degree at the same university.

His research interests include optical wavelength conversion and optical parametric amplifier in optical communication systems.



Changxi Yang received the B.S. degree in physics from Nankai University, Tianjin China, in 1986 and the Ph.D. degree in physics from the Institute of Physics, Chinese Academy of Sciences, Beijing, China, in 1992.

In 1992, he joined the Crystal Growth Group, Institute of Physics, Chinese Academy of Sciences. In 1994 and 1995, he was as a Visiting Scholar at the Department of Electrical and Computer Engineering, University of California, Santa Barbara. In 1996, he was an STA Fellow at the National Laboratory of Metrology, Tsukuba, Japan. In 1998, he was a Research Fellow at the Department of Physics, University of Exeter, U.K. In 1999 and 2000, he was with Bell Labs, Murray Hill, NJ, and the Department of Physics, University of Arkansas, Fayetteville, as a Senior Research Associate. He is currently a Professor at the Department of Precision Instruments, Tsinghua University, Beijing, China. His current research interests are photonic crystal fibers, frequency conversion with ultrashort pulses, polarization dispersion compensation, and optical fiber communications.